Matsumura, M., & Matthews, B. W. (1989) *Science 243*, 792–794.
Remington, S., Wiegand, G., & Huber, R. (1982) *J. Mol. Biol. 158*, 111–152.
Rossmann, M. (1979) *J. Appl. Crystallogr. 12*, 225–238.
Schmid, M. F., Weaver, L. H., Holmes, M. A., Gruetter, M. G., Ohlendorf, D. H., Reynolds, R. A., Remington, S. J., & Matthews, B. W. (1981) *Acta Crystallogr. A37*, 701–710.
Srere, P. A. (1966) *J. Biol. Chem. 241*, 2157–2159.
Srere, P. A. (1972) *Curr. Top. Cell. Regul. 5*, 245–283.
Tanaka, N. (1977) *Acta Crystallogr. A33*, 191–193.
Tronrud, D., Ten Eyck, L. F., & Matthews, B. W. (1987) *Acta Crystallogr. A43*, 489–501.
Weitzman, P. D. J., & Danson, M. J. (1976) *Curr. Top Cell. Regul. 10*, 161–204.
Wiegand, G., & Remington, S. (1986) *Annu. Rev. Biophys. Biophys. Chem. 15*, 97–117.
Wiegand, G., Remington, S., Deisenhofer, J., & Huber, R. (1984) *J. Mol. Biol. 174*, 205–219.

Assignments of Backbone ^1H, ^{13}C, and ^{15}N Resonances and Secondary Structure of Ribonuclease H from *Escherichia coli* by Heteronuclear Three-Dimensional NMR Spectroscopy

Toshio Yamazaki,*,‡ Mayumi Yoshida,§ Shigenori Kanaya,∥ Haruki Nakamura,∥ and Kuniaki Nagayama*,‡

Biometrology Lab, JEOL Limited, Musashino, Akishima, Tokyo 196, Japan, Tokyo Research Laboratories, Kyowa Hakko Kogyo Company, Limited, Machida, Tokyo 194, Japan, and Protein Engineering Research Institute, Furuedai, Suita, Osaka 565, Japan

Received January 7, 1991; Revised Manuscript Received March 20, 1991

ABSTRACT: The assignments of individual magnetic resonances of backbone nuclei of a larger protein, ribonuclease H from *Escherichia coli*, which consists of 155 amino acid residues and has a molecular mass of 17.6 kDa are presented. To remove the problem of degenerate chemical shifts, which is inevitable in proteins of this size, three-dimensional NMR was applied. The strategy for the sequential assignment was, first, resonance peaks of amides were classified into 15 amino acid types by ^1H–^{15}N HMQC experiments with samples in which specific amino acids were labeled with ^{15}N. Second, the amide ^1H–^{15}N peaks were connected along the amino acid sequence by tracing intraresidue and sequential NOE cross peaks. In order to obtain unambiguous NOE connectivities, four types of heteronuclear 3D NMR techniques, ^1H–^{15}N–^1H 3D NOESY-HMQC, ^1H–^{15}N–^1H 3D TOCSY-HMQC, ^{13}C–^1H–^1H 3D HMQC-NOESY, and ^{13}C–^1H–^1H 3D HMQC-TOCSY, were applied to proteins uniformly labeled either with ^{15}N or with ^{13}C. This method gave a systematic way to assign backbone nuclei (N, NH, $C^\alpha H$, and C^α) of larger proteins. Results of the sequential assignments and identification of secondary structure elements that were revealed by NOE cross peaks among backbone protons are reported.

Ribonuclease H (RNase H)[1] is an enzyme that cleaves the RNA moiety of an RNA–DNA hybrid endonucleolytically. It degrades an RNA strand into oligonucleotides with 5′-phosphate and 3′-hydroxyl termini with the aid of Mg^{2+} but is inactive with respect to other structures of nucleic acids, such as single- or double-stranded DNA and single- or double-stranded RNA. This function was first recognized in extracts from calf thymus (Stein & Hausen, 1969) and was later found in various organisms ranging from prokaryotes to higher eukaryotes (Crouch & Dirksen, 1982). The C-terminal domains of retroviral reverse transcriptases also have this function.

In the present study, RNase H from *Escherichia coli* has been investigated; this enzyme consists of 155 amino acid residues and has a molecular mass of 17.6 kDa (Kanaya & Crouch, 1983). A series of site-directed mutagenesis experiments (Kanaya et al., 1990) revealed the active site of this enzyme. Recently, a three-dimensional structure was proposed for the RNase H on the basis of X-ray crystallography data, at a 1.8-Å resolution (Katayanagi et al., 1990; Yang et al., 1990).

The nuclear magnetic resonance experiment has recently become one of the most efficient techniques for clarifying the structure–function relationship of proteins. For the atomic scale investigation of protein structures, each resonance peak in NMR spectra should first be assigned to a specific atom in the molecule. The assignment strategy for small proteins or peptides (<10 kDa) has been well-established (Wüthrich, 1986). The first step is the use of COSY to classify proton resonances into groups of amino acids according to the spin–spin coupling networks that reflect the amino acid chemical structures. The second step is the sequential connection of the classified spin systems along the primary structure. In most of the neighboring residues, pairs of protons, $C^\alpha H(i-1)$–$NH(i)$ [the proton at the α-carbon of $(i-1)$th residue and the amide

* To whom correspondence should be addressed.
‡ Biometrology Lab, JEOL Ltd.
§ Tokyo Research Laboratories, Kyowa Hakka Kogyo Co., Ltd.
∥ Protein Engineering Research Institute.

[1] Abbreviations: C^α, α-carbon; $C^\alpha H$, proton at the α-carbon; C^β, β-carbon; $C^\beta H$, proton at the β-carbon; $C^\gamma H_3$, methyl protons at the γ-carbon; COSY, two-dimensional correlation spectroscopy; HMQC, heteronuclear multiple-quantum correlation; N, backbone amide nitrogen; N^ϵ, ϵ-nitrogen; $N^{\epsilon 1}$, $\epsilon 1$-nitrogen; $N^\epsilon H$, proton at the ϵ-nitrogen; $N^{\epsilon 1}H$, proton at the $\epsilon 1$-nitrogen; NH, proton at the backbone amide nitrogen; NMR, nuclear magnetic resonance; NOE, nuclear Overhauser effect; NOESY, nuclear Overhauser effect spectroscopy; RNase H, ribonuclease H; ROE, rotating frame NOE; TOCSY, total correlation spectroscopy; TSP, 3-(trimethylsilyl)tetradeuteriopropionate; TMS, tetramethylsilane; amino acids are denoted by standard one- or three-letter codes.

0006-2960/91/0430-6036$02.50/0

proton of ith residue, respectively] or NH(i-1)–NH(i), are located close to each other. NOESY can extract these connectivities and affords the information for the individual assignments of resonances at the backbone of a protein molecule from the N- to the C-terminus.

As the protein size becomes larger, degenerate chemical shifts appear more often due to an increased number of resonance peaks and their broadened line widths. When it exceeds 10 kDa, unmanageable identification of spin–spin coupling networks and ambiguous sequential connection of resonances impair the strategy mentioned above. Note that cross peaks in NOESY spectra should have nondegenerate chemical shifts in both dimensions to be unambiguously traced. There have been two policies applied to remove this problem. One is to improve spectral resolution by increasing the applied magnetic field, and the other is to introduce new frequency axes to develop resonance peaks in the higher dimensional spectral space. We have employed the three-dimensional (3D) NMR technique, which was originally introduced as a homonuclear technique (Griesinger et al., 1987a) and applied to biological molecules (Griesinger et al., 1987b; Vuister et al., 1988, 1989; Oschkinat et al., 1988). Later, it was extended to heteronuclear 3D NMR (Fesik & Zuiderweg, 1988). The advantage of heteronuclear 3D NMR is the high ability to distinguish between degenerate proton resonances with chemical shifts of other nuclei, ^{13}C or ^{15}N, to which the concerned protons are covalently bonded, conserving the number and intensities of cross peaks, compared with those of the corresponding two-dimensional (2D) NMR.

As a quite new technique, triple-resonance 3D experiments specialized for the observation of sequential connection of backbone nuclei through direct J connectivities have been proposed. It is an unambiguous assigning procedure suitable for computer automation (Ikura et al., 1990), but it requires an extension of equipment.

In this study, a novel methodology with a combination of various kinds of 3D NMR was attempted at a relatively low field strength of 400 MHz. The standard procedure with a combination of COSY and NOESY 2D experiments was replaced by (1) ^{15}N–^1H HMQC for samples in which the amino acids were selectively labeled with ^{15}N, (2) ^1H–^{15}N–^1H 3D NOESY-HMQC, ^1H–^{15}N–^1H 3D TOCSY-HMQC, and chemical shift difference ^1H–^{15}N–^1H 3D NOESY for a sample uniformly labeled with ^{15}N, and (3) ^{13}C–^1H–^1H 3D HMQC-NOESY and ^{13}C–^1H–^1H 3D HMQC-TOCSY for a sample uniformly labeled with ^{13}C.

The ^1H–^{15}N HMQC experiments for the selectively labeled samples, in each of which amide nitrogens of a particular type of amino acid were labeled with ^{15}N, were performed to classify amide N–NH cross peaks by the types of amino acids. In these HMQC spectra, only amide cross peaks corresponding to the labeled amino acid appear, and they can be clearly identified with higher sensitivity.

The ^1H–^{15}N–^1H 3D NOESY-HMQC and ^1H–^{15}N–^1H 3D TOCSY-HMQC experiments for the sample uniformly labeled with ^{15}N were performed to trace sequential connectivities. In the ^{15}N 3D NOESY-HMQC spectra, two kinds of sequential connectivities, $C^\alpha H$–NH and NH–NH, were obtained. Intraresidue and interresidue $C^\alpha H$–NH cross peaks can be distinguished with the aid of ^{15}N 3D TOCSY-HMQC spectra as has been done with COSY experiments in the conventional approach. On the other hand, a single ^{15}N 3D NOESY-HMQC experiment suffices to resolve the NH–NH sequential connectivities. Applications of this kind of experiment to larger proteins have been reported (Marion et al., 1989a,b; Zuiderweg & Fesik, 1989a; Driscoll et al., 1990; Ikura et al., 1990b; Nagayama et al., 1990). When two sequential amides have a degenerate chemical shift, the NH–NH connectivities are identified by a chemical shift difference ^{15}N 3D HMQC-NOESY-HMQC experiment.

The ^1H–^{13}C 3D HMQC-NOESY and ^1H–^{13}C 3D HMQC-TOCSY experiments with the sample uniformly labeled with ^{13}C have been performed to resolve degenerate chemical shifts of $C^\alpha H$ protons, which have a narrower chemical shift dispersion than amide protons. The combination of these four 3D spectra can distinguish $C^\alpha H$–NH connectivities uniquely (Nagayama et al., 1990). In ^{13}C 3D experiments also, amide proton resonances should be observed in the detection period since they are apart from the troublesome water signal. The order HMQC-(NOESY or TOCSY) is thus chosen, contrary to the experiment of (NOESY or TOCSY)-HMQC for ^{15}N 3D NMR.

Several assignment procedures have been applied to proteins of a comparable size (~20 kDa) with great success by other groups. The labeling of proteins by specific amino acids, where carbonyl carbons and amide nitrogens are doubly labeled (Kainosho & Tsuji, 1982), provides correct information on the peptide connection. A combination with isotope labelings and isotope-edited 2D experiments gives an ability to assign proton resonances (Torchia et al. 1988, 1989; McIntosh et al., 1990). A set of isotope-edited 2D spectra obtained for many kinds of samples selectively labeled at various amino acid residues may have a similar resolving power to a 3D spectrum, but it is more time consuming to obtain its full set. The first report on assignment with ^{15}N 3D experiments was published recently (Driscoll et al., 1990). In an assignment study where backbone amides hold a special position, ^{15}N 3D experiments are very important as seen in this study.

The new techniques to assign the resonance peaks of backbone protons, nitrogens, and C^α carbons are fully described. This method has been applied to the assignments for resonances of backbone nuclei of *E. coli* RNase H. The secondary structure elements, α-helices and β-strands, and a core structure with a β-sheet identified with NOESY and TOCSY spectra are also reported.

Materials and Methods

Protein Preparation. *E. coli* N4830-1 with plasmid vector pPL801 controlled by the bacteriophage λ P_L promoter was utilized for the overproduction of RNase H (Kanaya et al., 1989). At 42 °C, production of the protein was induced after multiplication at 30 °C. This strain required His, Ile, Val, and two vitamins for its growth. For isotopic labeling, minimum culture medium (M9) was used. Amino acids (40 mg of His, Ile, and Val), vitamins (50 mg of D-Biotin and thiamine), and antibiotics (100 mg of ampicillin) were added to 1 L of culture. Growth in M9 was slightly slower than in L broth medium (LB), and the doubling time was 3 h. The 1-mL and 100-mL preculture took one day each. When the absorbance at 600 nm became 0.7~0.9, the temperature was raised. After the temperature reached 42 °C, cultivation was continued for 4 h at this temperature. The final absorbance was 1.5~1.8. Cells were then harvested by centrifugation and subjected to purification procedures as described previously (Kanaya & Crouch, 1983). About 15 mg of purified protein can be obtained from 1 L of culture.

^{15}N and ^{13}C Labeling. The protein sample, uniformly and fully labeled with ^{15}N, was prepared by cultivation of *E. coli* in the minimal medium with $^{15}NH_4Cl$ (99%) as the sole nitrogen source. Since [^{14}N]His, Ile, and Val were added in the medium, nitrogens of His residues were not labeled, Val

Table I: Culture Conditions for Selective Labelings with ^{15}N-Labeled Amino Acids and the Resultant Rates of Isotope Enrichments[a]

^{15}N-labeled amino acid	^{14}N-labeled amino acid (mg/L)	enrichment	cross labelings
G	H, I, V, L (40)	1	S, C (1/3); W (1/10)
L	H, I, V (40)	1/3	I (1/5); V, A (1/10)
A	H, I, V, L (40)	1/3	
D	H, I, V, L (40)	1/10	all others (1/10)
E	H, I, V, L (40)	1/8	all others (1/8)
F	H, I, V, L (40)	1/4	Y (1/4); all others (1/8)
H[b,c]	I, V, L (40)	1	
I[c]	H, V, L (40)	1/2	L (1/4); V, A (1/8)
K	H, I, V, L (40)	1	
M	H, I, V, L (40)	1	
T[b]	H, I, V, L (40)	1/2	G (1/4)
V[c]	H, I, L (40)	1/2	A (1/4)
C	H, I, V, L (40)	1	A (1/10)
E	all others (100)	1/8	A, N, D, Q, S (1/12)
S[b]	G, C, W (100); H, I, V, L (40)	1/4	G (1/4)
Y	E (100); H, I, V, L (40)	1/2	F (1/4); E, Q, A, D, N (1/10)

[a] The ^{15}N amino acids to be labeled and the normal ^{14}N amino acids were added at the beginning of induction. The approximate rates of desired labeling and undesired cross labelings were estimated from the intensity ratio of peaks observed in HMQC spectra. [b] DL-amino acid. [c] 40 mg/L for the initial medium; 60mg/L at induction.

residues were labeled at a very low rate, and Ile and Leu residues were labeled partially through metabolic leakage.

The protein sample, uniformly and fully labeled in ^{13}C, was prepared in the minimal medium with [^{13}C]glucose (98%) as the sole carbon source. His, Ile, Val, and Leu residues were not labeled since [^{12}C]His, Val, Ile, and Leu had to be added in the medium. Though Leu was not required for growth, [^{12}C]Leu was also added to prevent the partial cross labeling from Val. These four amino acids were additionally supplied at the beginning of induction.

A series of samples in which amino acids were selectively labeled with ^{15}N was prepared in the minimal medium with 100 mg/L of the corresponding ^{15}N-labeled amino acids (95–98%), which were added at the beginning of induction. After 2 h of induction, the cultivation was stopped to suppress cross labeling, though in the case of uniform labeling the cultivation was continued for 4 h or more. It gave half the yields of uniform labeling. Protein samples labeled with [^{15}N]Ala, Cys, Asp, Glu, Phe, Gly, His, Ile, Lys, Leu, Met, Ser, Thr, Val, or Tyr were prepared. For a few samples, counter ^{14}N-labeled amino acids against cross labeling were deliberately added together with the ^{15}N-labeled amino acids required for labeling to suppress the metabolic leakage. The conditions for each selective labeling are summarized in Table I.

NMR Spectroscopy. NMR experiments were carried out on a 400-MHz JEOL GSX400 spectrometer. The temperature of the samples was controlled at 27 °C. The samples were dissolved in a 0.1 M deuteriated acetate buffer of 80% H_2O/20% D_2O, pH 5.5. Exchange to the buffer solution and concentration were performed with a Centricon-10 (Amicon). Concentrations of proteins labeled with specific amino acids were about 1 mM, and those uniformly labeled with ^{15}N or ^{13}C were about 2 mM. Sample solutions of 0.25 mL were placed in 5-mm NMR microtubes BMS005 (Shigemi Standard Joint Ind Co., Ltd.) (Takahashi & Nagayama, 1988). The solutions were stable for several months at 4 °C.

Proton chemical shifts are relative to the water signal (4.78 ppm relative to TSP in the same buffer and at the same temperature). Carbon and nitrogen chemical shifts are calculated from the offsets; that of ^{13}C for dioxane (with ^{13}C 1D NMR) and that of ^{15}N of formamide (with ^{15}N–^1H HMQC) with an external lock of the same buffer were recorded and set to 67.9 ppm (^{13}C, relative to TMS) and 113.3 ppm (^{15}N, relative to liquid NH_3) after compensation of differences of the magnetic susceptibilities.

Two-Dimensional NMR. ^1H detected ^{15}N–^1H correlation experiments, HMQC (Bax et al., 1983), with a slight modification to incorporate solvent suppression, were performed on the samples selectively labeled with ^{15}N amino acids. Two kinds of solvent suppression techniques were employed. One was presaturation of the water signal by a DANTE pulse (Morris & Freeman, 1978). This technique was employed in the experiments for all samples. The other was filtered observation by a 1–1 echo pulse sequence, which was previously reported (Griffey et al., 1985a; Sklenar & Bax, 1987). This experiment was applied to samples where the ^{15}N enrichment was reduced by metabolic leakage. Both suppression techniques had their respectively disadvantages: the presaturation scheme affected not only the water signal but also resonances whose chemical shifts were close to that of water, and the saturation was transferred to others through spin diffusion; the 1–1 echo scheme had a narrower observation width. The 1–1 echo scheme, however, had the advantage that peaks were sharp because the J splittings by NH–C$^\alpha$H couplings in the ω_1 direction collapsed. This problem is also a major concern in 3D NMR. Experimental conditions were as follows: the carrier frequency of ^1H was set to that of the water signal, and that of ^{15}N was set to the center of the backbone amide nitrogen region; the spectral width for ^1H observation was 15 ppm (6000 Hz) and that for ^{15}N was 50 ppm (2000 Hz); the resolution for ^1H was 5.9 Hz and that for ^{15}N was 7.8 Hz; the maximum observation of the 1–1 echo filter was set to 8.78 ppm, which was 4.0 ppm below the carrier frequency; acquisition was repeated eight times for each t_1 value, leading to a total experimental time of about 2 h. Under these conditions, peaks of Arg N$^\epsilon$H protons were folded into the backbone amide region, but they were prevented from overlapping. For the samples labeled at a low rate, ^{15}N-Asp, Glu, Ser, and Phe, accumulation was continued overnight.

Three-Dimensional NMR. Four kinds of 3D NMR experiments were performed to obtain unambiguous sequential connectivities. In ^1H–^{15}N–^1H 3D NOESY-HMQC experiments, two solvent suppression techniques, presaturation and 1–1 echo, were employed for the same reasons as mentioned above. The pulse sequence with the 1–1 echo is shown in Figure 1a. The phase cycling of the refocusing pulse used in the HMQC part of the sequence was reduced from four phases to two, in order to reduce the experimental time. This phase cycling works properly only when it is combined with the HMQC scheme. The pulse sequence with presaturation was similar to that already reported (Marion, 1989). In these experiments, the magnetizations of neighboring protons were transferred to amide protons with the frequency labels of ^{15}N and ^1H; and then in the 3D spectra the cross peaks, NH(i–1)–NH(i), NH(i+1)–NH(i), C$^\alpha$H(i–1)–NH(i), and C$^\alpha$H(i)–NH(i), were aligned along the ω_1 direction. For the ^{15}N 3D TOCSY-HMQC experiments, which detected only the cross peaks corresponding to C$^\alpha$H(i)–NH(i) J connectivities, the pulse sequence shown in Figure 1b was used. The experimental conditions were as follows: the spectral offsets for ^1H and ^{15}N NMR were chosen to be the same as used in HMQC experiments; the spectral widths of the t_1 (^1H), t_2 (^{15}N), and t_3 (^1H) periods were set to 12 ppm (4800 Hz), 50

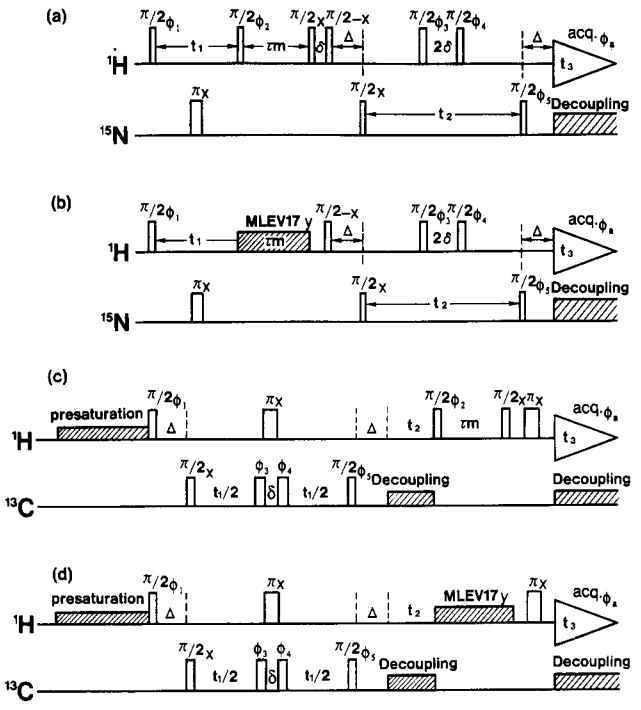

FIGURE 1: Pulse sequences of 3D NMR experiments. (a) ^1H–^{15}N–^1H 3D NOESY-HMQC. The fixed times were set as τ_m (the NOE mixing time) = 100 ms, $\Delta[1/(2^1J_{NH})$ where $^1J_{NH}$ was the coupling constant between N and H in Hz] = 5 ms, and $\delta[1/(4\omega_{opt})$ where ω_{opt} was the offset optimally observed with a 1–1 echo filter in Hz] = 156 μs. The phases of pulses were $\phi_1 = X$, $\phi_2 = [4X, 4(-X)]$, $\phi_3 = (2X,2Y)$, $\phi_4 = 2\ [2(-X), 2(-Y)]$, $\phi_5 = (X, -X)$, and $\phi_a = (X, -X, -X, X, -X, X, X, -X)$ for real–real signal of the experiment. $\phi_1 = Y$ was used for imaginary signal in the first dimension and $\phi_5 = (-Y, Y)$ was used for imaginary signal in the second dimension. WALTZ-16 was used for heteronuclear decoupling. (b) ^1H–^{15}N–^1H 3D TOCSY-HMQC. The fixed times were set as τ_m (the isotropic mixing time) = 30 ms, and others were the same as shown in (a). ROE-eliminated MLEV-17 with straddling spin lock pulses was used for isotropic mixing. The phases of pulses were $\phi_a = (X, -X, -X, X)$ and the others were the same as shown in (a). (c) ^{13}C–^1H–^1H 3D HMQC-NOESY. The fixed times were set as τ_m (the NOE mixing time) = 100 ms, $\Delta[1/(2^1J_{CH})$ where $^1J_{CH}$ was the coupling constant between C and H in Hz] = 3 ms, $\delta\ [(2n+1)/(2\omega_{dec})$ where ω_{dec} was the offset ^{13}C to be decoupled] = 125 μs. The carrier was set to the center of the C^α resonance frequencies, and carbonyl carbons were inverted for decoupling. The pulse widths should be 90° in an ideal case, but the pulse widths and interval were adjusted for the compensation of off-resonance effect. The phases of pulses were $\phi_1 = X$, $\phi_2 = [4X, 4(-X)]$, $\phi_3 = (2X, 2Y)$, $\phi_4 = [2(-X), 2(-Y)]$, $\phi_5 = (X, -X)$, and $\phi_a = [2(X, -X), 2(-X, X)]$ for real–real signals of the experiment. $\phi_1 = -Y$ was used for imaginary signals in the first dimension and $\phi_5 = (-Y, Y)$ was used for imaginary signals in the second dimension. (d) ^{13}C–^1H–^1H 3D HMQC-TOCSY. Isotropic mixing was made by the same composite pulse as used in ^{15}N experiment. The phases of pulses were the same as shown in (c) except $\phi_a = (X, -X)$.

ppm (2000 Hz), and 15 ppm (6000 Hz), respectively; the number of sampled complex points in the three directions was 128 (t_1), 32 (t_2), and 256 (t_3); the mixing time for NOESY was 100 ms, and that for TOCSY was 30 ms; TOCSY experiments with longer mixing times (60 and 90 ms) gave peaks only for Ala $C^\beta H_3$'s and for protons on some mobile side chains.

In the ^{13}C 3D NMR experiments, a new problem arose. Since the sample was enriched uniformly and fully with ^{13}C, not only C^α carbons but also β-carbons (C^β) and carbonyl carbons (C′) were labeled with ^{13}C. This brought about ^{13}C homonuclear couplings and modulation of chemical shifts of C^α carbons, causing both low resolution and poor sensitivity. To get rid of the difficulties, we modified the original sequence (Fesik & Zuiderweg, 1988), as shown in Figure 1c for the ^{13}C 3D HMQC-NOESY experiments. Note that selective inversion by a 1–1 pulse was added to the HMQC part (t_1). It worked as a 0° pulse for C^α carbons and as a 180° pulse for C′ and C^β carbons. For this experiment, only presaturation solvent suppression was adopted. But even $C^\alpha H$ protons just under the water signal did not vanish, because they were split by large ^{13}C–^1H spin–spin couplings (Griffey et al., 1985b). Spin echo pulses were added immediately before acquisition to avoid the transient effect of the low-pass filter (Davis, 1989). In this spectrum, NH(i)–$C^\alpha H(i)$ and NH(i+1)–$C^\alpha H(i)$ were aligned along the ω_3 direction. A ^{13}C–^1H–^1H HMQC-TOCSY experiment was also performed to distinguish intraresidue NH–$C^\alpha H$ cross peaks. The pulse sequence is shown in Figure 1d. The experimental conditions were as follows: the conditions for ^1H were the same as used in the ^{15}N 3D experiments; the carrier frequency of ^{13}C was set to the center of C^α resonances, the spectral width was 50 ppm (5000 Hz), the number of complex points sampled with 64, and the mixing time was 100 and 30 ms for NOESY and TOCSY, respectively.

Chemical Shift Difference Three-Dimensional NMR. In the above 3D NMR experiments, a connectivity between two protons was evolved by the chemical shift of the heteronucleus to which one of the protons was attached. Two cross peaks and two diagonal peaks appeared in the spectra. One of the two diagonal peaks and one of the two cross peaks had the same heteronuclear chemical shift, and the other cross and diagonal peaks also had another chemical shift. If the chemical shifts of the two protons were degenerate, the diagonal and cross peaks were overlapped. The information of the connectivity was lost. This situation occurred in the amide–amide region of the ^{15}N 3D NOESY experiment.

A new experiment was devised to recover these connectivities, which were essential for sequential assignment. In this experiment, NOE cross peaks between NH–N(i) and NH–N(j) were evolved by three frequencies, the chemical shift of NH(i), that of NH(j), and the difference of the chemical shifts of N(i) and N(j). In the spectrum, all diagonal peaks gathered to the central plane where the difference of chemical shifts of nitrogens was zero. On the other hand, cross peaks between two amides were scattered in 3D space in general. A cross peak between amides whose proton chemical shifts were degenerate but whose nitrogen chemical shifts were different from each other appeared in a different slice apart from the diagonal peaks.

The pulse sequence used in this experiment consisted of five periods as shown in Figure 2. On both sides of the NOE mixing τ_m period, there were ^{15}N and ^1H evolution periods where the signal was modulated by the chemical shifts of both NH and N of both interacting amides. The ^1H evolution and the ^1H acquisition corresponded to t_1 and t_3, respectively. But in order to obtain only differences of chemical shifts of ^{15}N's, both ^{15}N evolution times were bound to an increasing time t_2. By a combination of pulse phases, sine or cosine modulation of each evolution was selected. Four different types of modulated signals along t_2, c_ic_j, c_is_j, s_ic_j, and s_is_j were recorded [where $c_i = \cos[\omega(N_i)t_2]$, $c_j = \cos[\omega(n_j)t_2]$, $s_i = \sin[\omega(n_i)t_2]$, and $s_j = \sin[\omega(N_j)t_2]$]. The signal obtained with the combination $(c_ic_j + s_is_j) + i(s_ic_j - c_is_j) = \exp[i[\omega(N_i) - \omega(N_j)]t_2]$ mimicked a modulation by a difference frequency of $\omega(N_i) - \omega(N_j)$ in t_2. The ^1H carrier was set to the center of amide proton region. The solvent signal was eliminated by presaturation with DANTE. The spectral widths and data points were 6 ppm/64 for the t_1 period, 100 ppm/32 for t_2, and 15

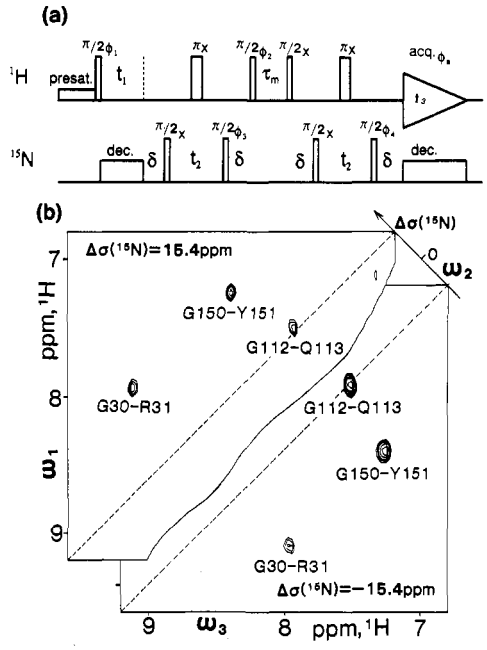

FIGURE 2: Shift difference 3D experiment. (a) Pulse sequence. The constant times were set as δ [$1/(2^1J_{NH})$] = 5 ms and τ_m (the NOE mixing time) = 200 ms. The phases of pulses were $\phi_1 = X$, $\phi_2 = [8X, 8(-X)]$, $\phi_3 = [2X, 2(-X), 2(-Y), 2Y]$, $\phi_4 = [2(X, -X), 2(-Y, -Y)]$, and $\phi_a = [2(X, -X, -X, X), 2(-X, X, X, -X)]$ for real–real signals. $\phi_1 = (-Y)$ for imaginary signals in the first dimension, and $\phi_4 = [2(-Y, Y), 2(-X, X))$ for imaginary signals in the second dimension. (b) In the 3D spectrum, the first (ω_1) and third (ω_3) dimensions show chemical shifts of interacting amide protons and the second one (ω_2) shows differences of chemical shifts of two amide nitrogens attached to the interacting protons. Partial 2D spectra sliced at a positive offset and at the corresponding negative offset in ω_2 are shown. Two cross peaks from an NOE connectivity can be observed at the symmetrical positions in the slices. The G112–Q113 cross peaks are very close to the diagonal line (indicated with the broken lines) but are not overlapped by diagonal peaks that fell onto the central plane (ω_2 = 0).

ppm/256 for t_3. The mixing time was 200 ms. The total experimental time was two days. Alternative experiments more sensitive but not easier to interpret have been reported by other groups (Ikura et al., 1990c; Zuiderweg et al., 1991).

Data Processing. 3D spectra of ^{13}C and ^{15}N were recorded and stored as sets of homonuclear 2D spectra modulated by heteronuclear chemical shifts. Each 2D FID was zero filled and Fourier transformed in both dimensions, and then a particular region (NH or $C^{\alpha}H$) was saved to the disk. These 2D spectra were read as a series of 1D spectra, transposed, and Fourier transformed. For all 2D and 3D spectra, the postacquisition solvent suppression technique was applied (Kuroda et al., 1989). The baseline rolling caused by this processing was avoided by opening the receiver gate early enough and starting the acquisition of data at the refocusing point, when all signals were in the same phase. Spin echo sequences were suitable for this experiment. The 2D spectra sliced from a 3D spectrum at each heteronuclear chemical shift were plotted out to process the successive spectral analysis of spin identification, sequential connection, and so on. The data processing, calculation, display, and plotting were all carried out on a μ-VAX II (DEC) with the software extended from TOOLKIT (the Rawland Institute for Science).

RESULTS

Amino Acid Identification. A total of 16 samples labeled with 15 different ^{15}N amino acids were prepared. ^1H–^{15}N HMQC spectra of these samples were compared with the spectra of the sample uniformly labeled with ^{15}N. Some of them were labeled only at the specific amino acids, but most of them were cross labeled at the different amino acids metabolically connected through transaminations or transformations.

Almost no metabolic leakage was observed in Met, Lys, Cys, and His labelings, and these amino acid residues in the protein were fully enriched with ^{15}N. On the contrary, Asp and Glu labeling diffused to most of the other amino acids and failed to distinguish themselves from others. The trick for [^{15}N]Glu labeling, where all the other ^{14}N-labeled amino acids except Glu and Pro were added at the induction, improved the results, and Glu peaks were successfully distinguished. In the [^{15}N]Phe labeling, Phe was cross labeled to Tyr at the same rate, while in the Tyr labeling a difference in the peak intensities between them was observed. Both Tyr and Phe were then identified. The results are summarized in Table I together with their culture conditions.

Peaks in the HMQC spectra of the uniformly labeled sample were primarily classified into the backbone amides of Ala, Cys, Glu, Phe, Gly, His, Ile, Lys, Leu, Met, Ser, Thr, Val, Tyr, other amino acids (Asp, Asn, Gln, Arg, or Trp), and the side-chain amides of Gln or Asn or the ring $N^{\epsilon 1}H$–$N^{\epsilon 1}$ of Trp. Peaks of $N^{\epsilon}H$–N^{ϵ} of Arg appeared in a distant area (80∼90 ppm, ^{15}N). An HMQC spectrum with the amide identifications is shown in Figure 3.

RNase H has three Cys residues, but only two peaks appeared in the HMQC spectra. Various experimental conditions (7∼47 °C, pH 3.5∼5.5) were tested to recover the missing resonance, but it never appeared. We observed the missing peak when RNase H was partially denatured by 0.1 M perdeuteriated dodecyl phosphocholine (purchased from TRC).

Sequential Assignment. In order to assign resonances to individual backbone nuclei, we used NOE connectivities between protons in neighboring residues. There are two major kinds of sequential connectivities. One is a strong NOE cross peak between $C^{\alpha}H(i)$ and NH(i+1) typically seen in β-strands. The other is an NOE cross peak between NH(i) and NH(i+1) typically seen in α-helices. In the statistical analysis of protein structures from the protein data bank, 98% of the pairs of close (<2.4 Å) $C^{\alpha}H$ protons and NH protons were sequential ones, and 88% of pairs of close (<3.0 Å) NH protons were also sequential ones (Billeter, 1982).

To make up for the lack of isotopic labeling of Val and His residues in the samples of the uniformly labeled protein, ω_2 ^{15}N-selected NOESY spectra of [^{15}N]Val-labeled samples and [^{15}N]His-labeled samples were taken and added to the ^{15}N 3D NOESY spectrum as two extra 2D spectral slices. An ω_2 ^{14}N-selected TOCSY spectrum of the sample uniformly labeled by ^{15}N, except at Val and His residues, was also taken and added to the ^{15}N 3D TOCSY spectrum as an extra 2D spectral slice. An ω_1 ^{12}C-selected NOESY spectrum of the sample uniformly labeled by ^{13}C except at His, Ile, Leu, and Val residues was taken and used as another slice in the ^{13}C 3D NOESY spectrum. The ^{13}C 3D TOCSY spectrum need not be afforded by extra slices of ^{12}C-selected TOCSY because those corresponding to His, Ile, Leu, and Val residues can be made from cross peaks observed in the ^{15}N 3D TOCSY spectrum.

The first kind of sequential assignment was performed based on the strong NOE cross peaks of $C^{\alpha}H(i)$–NH(i+1). A NH(i)–N(i)–$C^{\alpha}H(i)$ cross peak in the ^{15}N 3D TOCSY spectrum and a NH(i)–$C^{\alpha}H(i)$–$C^{\alpha}(i)$ cross peak in the ^{13}C 3D TOCSY spectrum were combined; and a strong $C^{\alpha}H$-(i)–$C^{\alpha}(i)$–NH(i+1) cross peak in the ^{13}C 3D NOESY spec-

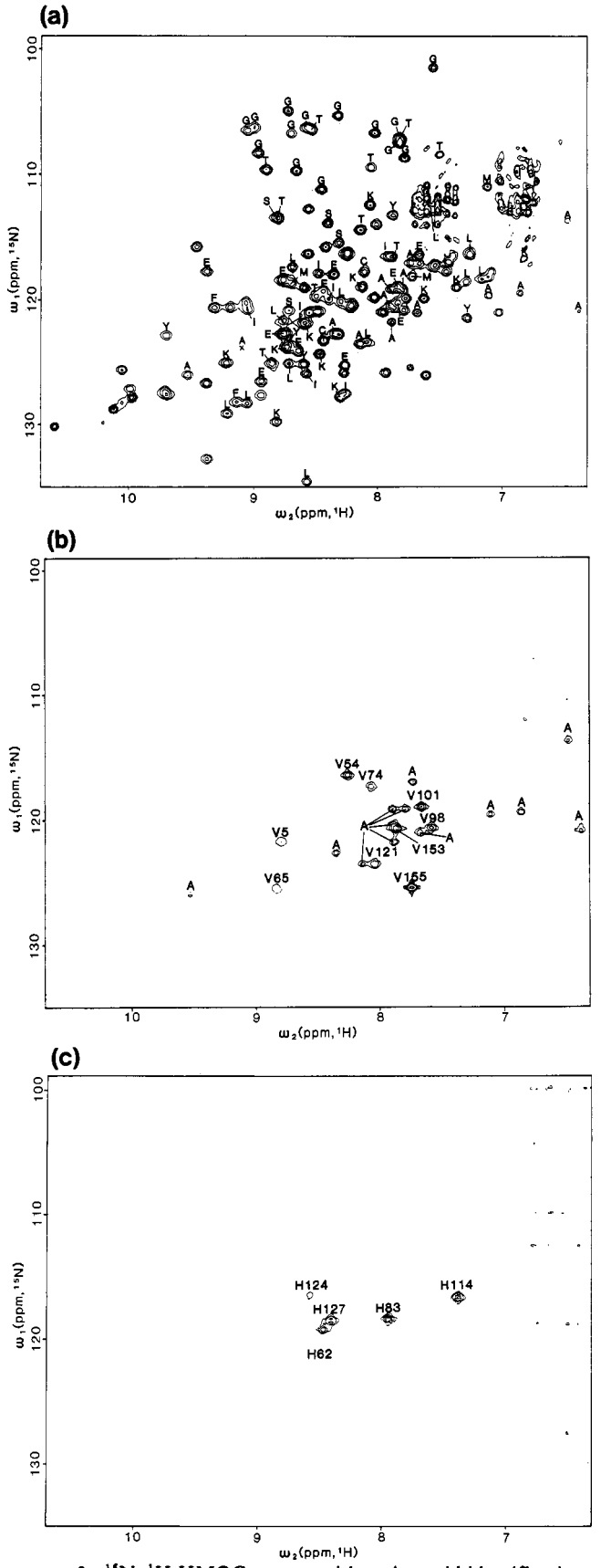

FIGURE 3: ^{15}N–^1H HMQC spectra with amino acid identifications for amides obtained by selective labeling. (a) Identification of 12 amino acids, except His and Val, is shown on a ^{15}N HMQC 1–1 echo spectrum of the ^{15}N uniformly labeled sample. (b) An HMQC spectrum of the [^{15}N]Val-labeled sample. Residue numbers assigned to the peaks from the Val residues are shown. The cross labeled Ala residues are also identified. (c) An HMQC spectrum of the [^{15}N]-His-labeled sample. The residue number assigned to the peaks from five His residues are shown.

trum and a strong $C^\alpha H(i)$–$NH(i+1)$–$N(i+1)$ cross peak in the ^{15}N 3D NOESY spectrum were combined. They were connected along the peptide backbone to the ends of these kinds of connectivities, Pro residues, or doubly degenerate chemical shifts that could not be resolved even by 3D NMR. Four long sequences of peaks were extracted. Their amino acid types, obtained with the selective-labeling experiments, were unambiguously matched to the specific parts of amino acid sequence. They were K3–G11, A24–G30, R31–A37, and K117–G123. An additional 12 shorter sequences of peaks were also obtained. Ten of them were unambiguously assigned because they were uniquely matched. After the assignments of these segments, they were extended to longer ones according to the amino acid sequence. Finally, they formed five long and six short segments.

L2–N16. At first, K3–G11 was a long sequence of resonance peaks connected unambiguously by strong NOESY and clear TOCSY cross peaks. The pattern of amino acids "-(K:Y)oVE(I:K)FToG" ["o" denotes amino acids other than those obtianed by the selective-labeling experiments, "(x:y)" indicates x or y] was uniquely matched to K3–G11. Moreover, there was a short segment of connected resonances with a sequence "(S:T)CL(G:T)", which was uniquely matched to S12–G15. The connectivity between G11 and S12 was not determined by intraresidue TOCSY and strong sequential NOESY cross peaks. The TOCSY peaks of G11 were too weak to be observed, and the sequential NOESY peaks between $C^\alpha H$(G11) and NH(S12) were weaker than other sequential NOESY peaks. The chemical shift of one of two $C^\alpha H$ protons was over 5 ppm. These were typically seen in the case of Gly residues in β-strands. The chemical shifts of two $C^\alpha H$ protons and C^α were determined by intraresidue NOESY cross peaks in ^{13}C 3D NOESY, where C^α's of Gly residues had distinct chemical shifts. This segment was extended to NH of L2, though the chemical shift of $C^\alpha H$ was same as that of an Ile residue. Two chemical shifts of the $C^\alpha H$ protons of G15 were determined by ^{13}C 3D TOCSY, though G15 and a Thr residue were overlapped on the ^{15}N–^1H HMQC plane. The chemical shifts of NH, N, $C^\alpha H$, and C^α of N16 were determined through strong NOESY and TOCSY peaks.

G20–G30. A24–G30 were connected by strong sequential NOESY cross peaks and strong TOCSY cross peaks, had an amino acid sequence "AILoYoG", and were matched uniquely to this part. There were three Gly residues in the preceding part. They had the same character mentioned above. They were extended from A24 up to G20 without ambiguity. The $C^\alpha H$–C^α J connectivity of G30 was also determined by ^{15}N 3D TOCSY and ^{13}C 3D TOCSY without ambiguity.

R31–T40. R31–A37 was also an unambiguous sequence with amino acids "oEKTFSA" and was uniquely matched. The connectivity between G30 and R31 was also observed in both manners, $C^\alpha H(i)$–$NH(i+1)$ and $NH(i)$–$NH(i+1)$. The connectivity between A37 and G38 was not distinguishable from an unassigned peak in ^{13}C and ^{15}N 3D spectra. Because the two NOESY cross peaks had the same NH and $C^\alpha H$ chemical shifts and similar strengths, only one led to a Gly residue and it was assigned to G38. Another short segment with amino acids "Y(S:T)" was uniquely assigned to Y39 and T40. The connectivity between G38 and Y39 was also observed in the ^{13}C 3D NOESY spectrum. The $C^\alpha H$ of T40 was determined by ^{15}N 3D TOCSY and ^{13}C 3D TOCSY. These connectivities, R31–T40, are shown in the spectra stripped and rearranged from the four 3D spectra in Figure 4.

E64–T69. The sequence of resonances with two amino acids "ST" was uniquely assigned to S68 and T69. The chemical

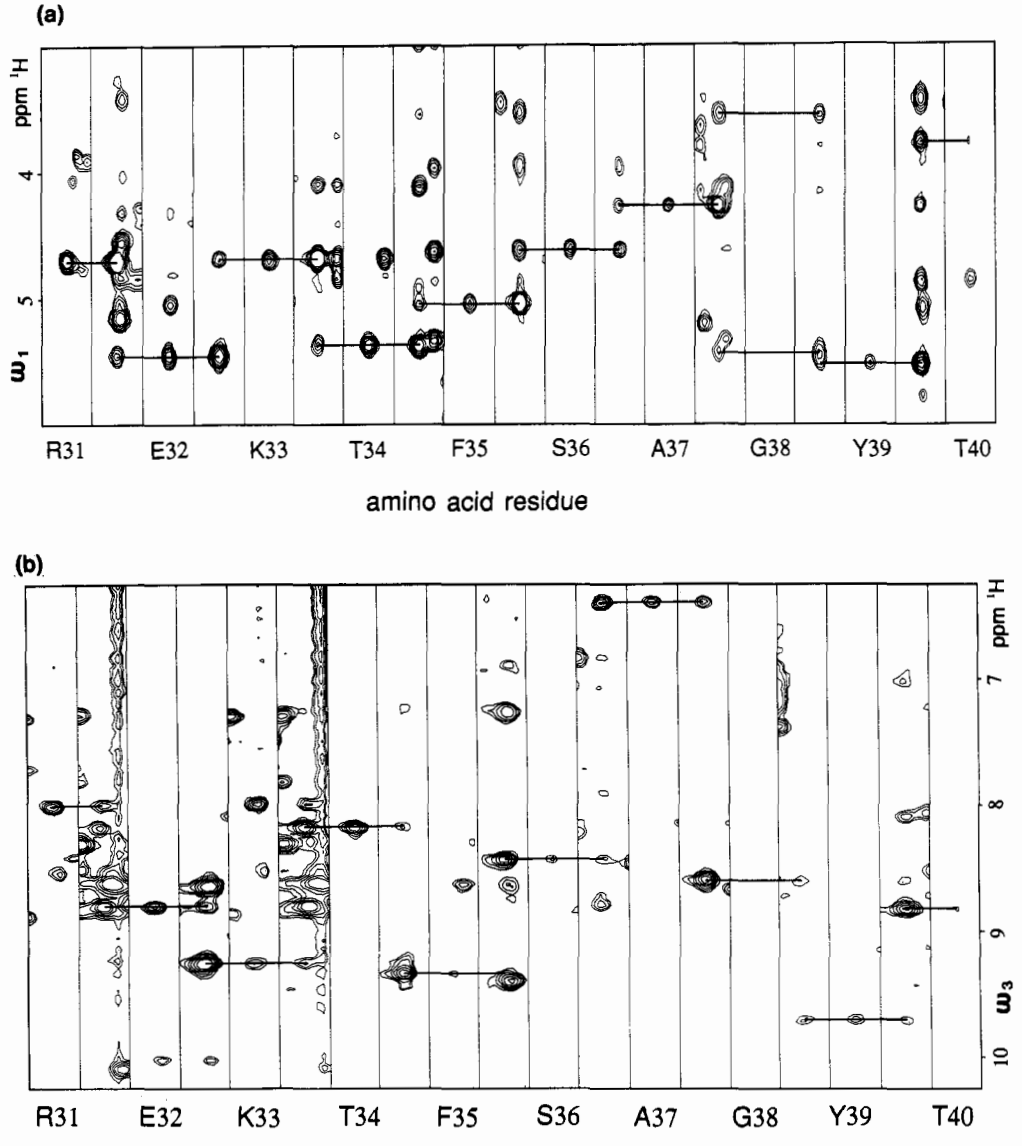

FIGURE 4: $C^{\alpha}H(i)$–NH(i+1) connectivities revealed for the sequence R31–T40 in the fingerprint region of RNase H 3D spectra. (a) ^{15}N 3D TOCSY-HMQC 1–1 echo and ^{15}N 3D NOESY–HMQC 1–1 echo spectra were stripped at the chemical shifts of amide nitrogens (ω_2) and amide protons (ω_3) into slices with narrow widths in ω_3 and rearranged in the order of the amino acid sequence. The two spectra sliced from TOCSY and NOESY are aligned alternately. The strips designated with residue names are from 3D TOCSY-HMQC, and the strips without the names are from 3D NOESY-HMQC. The intraresidue cross peaks appearing in NOESY and TOCSY and the sequential cross peak appearing in NOESY for each residue were connected. A TOCSY spectrum for G38 is not shown because no cross peak was observed. TOCSY and NOESY spectra of A37 are from ^{15}N 3D experiments with presaturation. (b) ^{13}C 3D HMQC-TOCSY and ^{13}C 3D HMQC-NOESY spectra were stripped at the chemical shifts of α-carbons (ω_1) and α-protons (ω_2) into slices with narrow widths in ω_2 and rearranged in the order of the amino acid sequence. A TOCSY spectrum of G38 is not shown.

shift of $C^{\alpha}H$–C^{α} of T69 was determined by ^{15}N 3D TOCSY and ^{13}C 3D TOCSY. Degenerate shifts at four positions had to be overcome to extend this short segment. The first one was degeneracy of $C^{\alpha}H$'s of L67 and V65, and both had strong sequential NOESY peaks. But they were distinguished by their amino acid types, and L67 was assigned. The $C^{\alpha}H$ of I66 was degenerate again to a His residue. These were also resolved by their amino acid types. Next, V65 mentioned above was assigned. The sequential NOESY connectivities G11–S12 and E64–V65 were also degenerate. Here, E64 was assigned without ambiguity because G11–S12 was already assigned and their amino acids were different.

H114–G123. The sequence of resonances with seven amino acids "KoEoVKG" was uniquely assigned to K117–G123. The shorter sequence with amino acids "HoI" was also uniquely assigned to H114–I116. There was a strong NOESY cross peak between I116 and K117. But $C^{\alpha}H$ of I116 had the same chemical shift as $C^{\alpha}H$ of L2. At this stage, L2 was already assigned and then I116 was assigned without ambiguity. $C^{\alpha}H_2$–C^{α} of G123 was also determined by ^{15}N 3D TOCSY and ^{13}C 3D TOCSY.

There were other segments assigned by using strong sequential $C^{\alpha}H$–NH cross peaks. Four residues of "EoTG" were assigned to E140–G150 and extended to L146 whose $C^{\alpha}H$ was overlapped by I66. $C^{\alpha}H_2$–C^{α} of G150 was observed in ^{15}N 3D TOCSY and ^{13}C 3D NOESY. R41 and T42 were assigned next. This segment had a pattern of amino acids "oT". This pattern matched to two parts on the primary structure, but the alternative position of D148–T149 was already assigned. $C^{\alpha}H$–C^{α} of T42 was observed in both ^{15}N and ^{13}C 3D TOCSY spectra. L59–H62 was assigned even though the sequential NOE between L59 and K60 was overlapped with

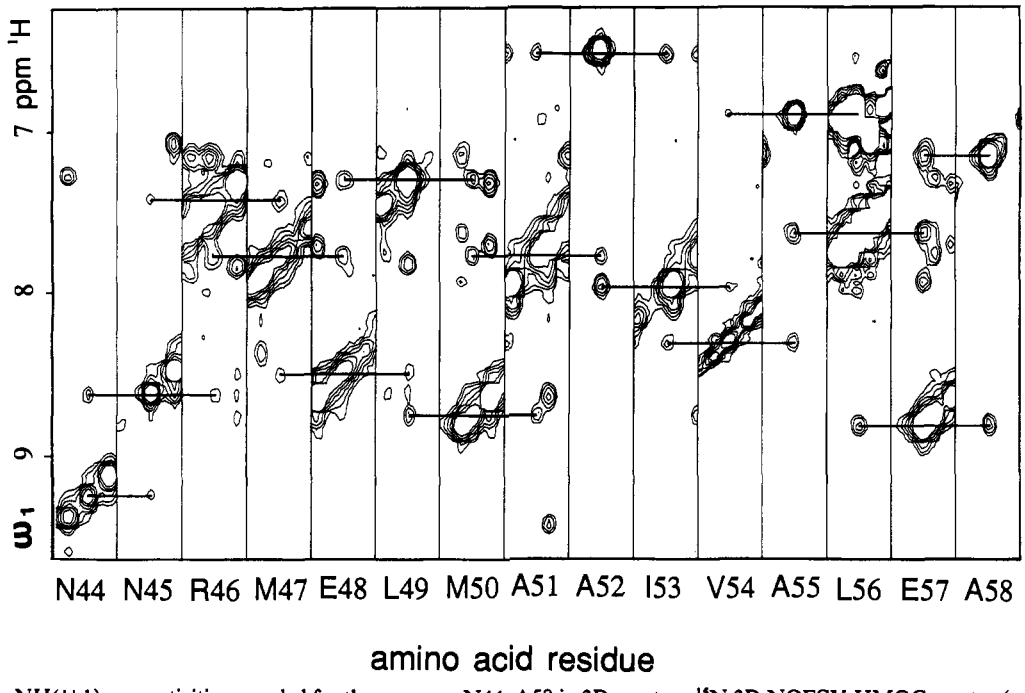

FIGURE 5: NH(i)–NH(i+1) connectivities revealed for the sequence N44–A58 in 3D spectra. ^{15}N 3D NOESY-HMQC spectra (with presaturation) were stripped and rearranged in the same manner as shown in Figure 4a. The diagonal peak, cross peak to the preceding residue, and cross peak to the next residue for each residue are connected. The spectrum of V54 is from ω_2 ^{15}N-selected 2D NOESY.

that between A37 and G38. W90–T92 including $C^\alpha H$–C^α of T92, V98–N100, and A125–H127 including $C^\alpha H$ of H127 were also assigned independently. Two short segments connected by strong NOESY peaks were left unassigned. Their patterns of amino acids were "To" and "KK", which appeared more than once in the unassigned parts of the amino acid sequence.

Five residues at the C-terminus, Y151–V155, seemed to be mobile. Both strong NOESY peaks between $C^\alpha H(i)$–NH(i+1) and NH(i)–NH(i+1) were observed. These resonances were easily assigned because their lines were very sharp.

The second kind of sequential connectivities were NOESY cross peaks between NH(i) and NH(i+1). The first task was to make pairs of NH(i)–N(i)–NH(i+1) and NH(i)–NH(i+1)–N(i+1) cross peaks in ^{15}N 3D NOESY spectrum. Cross peaks closer than 0.2 ppm to diagonal peaks were very hard to recognize. Three cross peaks buried under the diagonal peaks were observed in the spectrum of the chemical shift difference 3D NOESY. They were assigned to K87–R88, W104–Q105, and G112–Q113 as explained below (G112–Q113 is shown in Figure 2).

A total of 6 long and 11 short segments of cross peaks were extracted unambiguously in the ^{15}N 3D NOESY spectrum. Among them, two short segments were coincident with the previously assigned fragments K60–E61 and G126–H127. The rest of the sequences were compared with the primary structure by taking the indefinite directionality of connectivities into account, and they were assigned if the pattern appeared only once. And they were extended and connected to each other by overcoming the degeneracy. Finally, three long sequences and seven short segments were assigned. $C^\alpha H$ and C^α were left unassigned in the early stage of this assignment procedure.

N44–A58. Six NH and N pairs connected by NOESY cross peaks that had an amino acid pattern "oooME" were matched only to N44–E48 and assigned. Nine NH and N pairs with the sequence "MAAIVAL(E:o)A" were assigned to M50–A58. NOESY cross peaks between NH of E48 and L49 and between L49 and M50 were also observed, but NH–N of L49 was overlapped by an amino acid residue whose type was not known. These connectivities, N44–A58, are shown in the spectra stripped and rearranged from ^{15}N 3D NOESY in Figure 5.

Q72–K91. Five NH and N pairs with the sequence "oYVoo" were uniquely assigned to Q72–Q76, and six pairs of NH and N with the sequence "ooIHoo" were also uniquely assigned to Q80–W85. NH–NH sequential connectivities from Q76 to G77 and from Q80 to T79 were observed, and both NH and N chemical shifts of G77 and T79 were degenerate; a cross peak between I78 and G77 and/or T79 was observed. To make clear whether two cross peaks were overlapped in 3D space or either cross peak existed, ^{15}N-selected 2D NOESY spectra of a [^{15}N]Gly sample and a ^{15}N-labeled all-except-Gly sample were recorded. In both spectra the cross peaks were observed. A string of six residues "KKoGoK" matched to K86–K91 where W90–K91 was already assigned by strong $C^\alpha H(i)$–NH(i+1) NOESY peaks. NH–H of R88 was degenerate to that of L49, but it was assigned before, and hence this connection became unambiguous. The connectivity between W85 and K86 was not observed because both NH and N chemical shifts were close.

N100–H114. First, a sequence of resonances with a pattern "oAALGoH" was assigned to D108–H114 where H114 was already assigned. Next, a sequence with a pattern "oLoooL" was matched to D102–L107 or L103–D108. But they were assigned to D102–L107 since D108 was already assigned. The cross peaks between D102 and V101 were observed overlapped in the NH–NH 2D plane, but they could be distinguished by amino acids. The connectivity could be extended to N100, which was already assigned. The connectivity between them was not recognized because L107 and E108 had closer chemical shifts of both NH's and N's.

Other short segments were also assigned. Two residues of "KK" were assigned to K95–K96 because alternative position K86–K87 was already assigned, and the direction was also determined by a strong NOESY peak between $C^\alpha H$(K95) and NH(K96). Two residues of "EL" were also assigned to E135–L136 because all other possible positions were already assigned. Three residues of "AMo" were assigned to A141–

N143 independently. Two residues of "TL" were also assigned to T145–L146 where L146 was already assigned. Four segments of "Eo", "Co", and two "oA" remained unassigned at this stage.

Two strong $C^{\alpha}H(i)$–$NH(i+1)$ sequential connectivities left unassigned were assigned with the aid of NH–NH sequential connectivities. One was K95–K96 mentioned above. The other was T43–N44 because NH–N of N44 was assigned.

At this stage, only 17 NH and N pairs remained unassigned. Among them Gly, Ser, and His residues appeared only once. They were assigned to G18, S71, and H124, respectively, and according to the NH–NH NOESY peak of "Co", which was assigned to R132–C133 or C133–D134, C133 was assigned anyway. The invisible Cys resonance was assigned to C63. No more residues could be assigned by using the above characteristic NOE connectivities. The remaining 12 residues were assigned to fulfill short-range NOE connectivities.

It was expected that NOE cross peaks between $C^{\alpha}H(i)$ and $NH(i+1)$ could be observed in most cases. From the $C^{\alpha}H$ and C^{α} pair of T69 already assigned through the medium strength of NOESY peak in ^{13}C and ^{15}N 3D NOESY spectra, the NH and N pair of D70 was assigned. From the $C^{\alpha}H$ and C^{α} pair of T92 through the medium strength of NOESY peak, A93 and D94 connected by a NH–NH NOESY peak were assigned. The other NH–NH NOE connectivity of "oA" could be assigned to A137–R138 or R138–A139. In both cases R138 was assigned. Among three unassigned Ala residues, there existed only one NH–N to which a NOESY cross peak from $C^{\alpha}H$–C^{α} of R138 was observed. This was assigned to A139.

It was dangerous to assign the remaining parts by using $C^{\alpha}H(i)$–$NH(i+1)$ NOESY cross peaks because $C^{\alpha}H(i)$–$NH(i+3)$ or $C^{\alpha}H(i)$–$NH(i+4)$ NOESY cross peaks typically seen in α-helices were observed and they might lead to mistakes.

Two Ala residues could be assigned to A137 or A140. A NOESY $C^{\alpha}H$(A)–NH(R138) cross peak was observed, and it should be interpreted as $C^{\alpha}H$(A137)–NH(R138) not as $C^{\alpha}H$(A140)–NH(R138). The Ala residue was assigned to A137; the other was assigned to A140. There were five possibilities for assigning the remaining segment of E129–D134 to fulfill the amino acid types and the NH–NH sequential connectivities. Owing to the three facts that $C^{\alpha}H$(E131)–NH(R132) and $C^{\alpha}H$(E129)–NH(R132) connectivities existed and $C^{\alpha}H$(N130)–NH(E129) did not exist, a single answer was obtained. The difficulty in assignment of these parts was caused by their densely crowded chemical shifts. Among them, the shift degeneracy of E131 and E135 backbone nuclei was very severe, the chemical shifts of NH protons, $C^{\alpha}H$ protons, and C^{α} carbons were too close to distinguish, and the chemical shifts of N nitrogens were also close to each other.

A total of 65 $C^{\alpha}H$ and C^{α} pairs were left unassigned at this stage even though the NH and N of the residues were assigned. By ^{15}N 3D TOCSY and ^{13}C 3D TOCSY spectra, 52 of them were identified unambiguously and 13 were identified with the help of 3D NOESY spectra. For R75, W85, A93, N100, and W104, intraresidue cross peaks were observed only in the ^{15}N 3D TOCSY spectrum. For all except W85, intraresidue NOESY cross peaks were not degenerate in the ^{1}H–^{1}H 2D plane, and the chemical shifts were determined without ambiguity. But the chemical shifts of W85 and N84 were too close to distinguish, and the intraresidue NOESY peak of W85 and $C^{\alpha}H$(N84)–NH(W85) were overlapped in the ^{15}N 3D NOESY spectrum, and they corresponded to two peaks in the ^{13}C 3D NOESY spectrum. One was at C^{α}(N84), and the other was at a position that had not been assigned to any $C^{\alpha}H$ and C^{α} pair. The latter was assigned to C^{α}(W85). Among the eight remainders, $C^{\alpha}H$ and C^{α} pairs of N44, N45, A51, V54, S71, I82, and D108 were assigned by the clear NOESY cross peaks. $C^{\alpha}H$ of V74 was determined by the COSY and relayed COSY spectra in which $C^{\alpha}H$, $C^{\beta}H$, and $C^{\gamma}H_3$ protons of Val and Ile residues were seen.

To ascertain these assignments, NOESY $C^{\alpha}H(i)$–$NH(i+1)$ cross peaks were also checked. The cross peaks were observed in 48 cases. For M47–E48, V74–R75, I82–H83, and T145–L146, the NOESY peaks were not observed. The others could not be discussed because of degeneracy.

The chemical shifts of $C^{\alpha}H$ and C^{α} nuclei of residues whose NH protons were never observed, the N-terminus, five Pro residues, and C63, were determined as follows: The $C^{\alpha}H$ and C^{α} pairs of P17, P19, P97, P144, and C63 were assigned through strong NOESY cross peaks between $C^{\alpha}H(i)$–$NH(i+1)$ in the ^{13}C 3D NOESY and ^{15}N 3D NOESY spectra. The $C^{\alpha}H$ and C^{α} of N-terminus M1 were also identified by the sequential NOE $C^{\alpha}H$(M1)–NH(L2) with the medium strength of peak and led to an unassigned pair of $C^{\alpha}H$–C^{α}. For the last residue, P128, the sequential NOE $C^{\alpha}H$–(P128)–NH(E129) was very weak and observed only in the ^{15}N 3D NOESY spectrum. But the short-range $C^{\alpha}H$–(P128)–NH(E131) NOE was also weak but observed in the ^{13}C 3D NOESY spectrum. This was an unassigned position. The results of assignments for ^{1}H, ^{13}C, and ^{15}N resonances are summarized in Table II.

Discussion

Secondary Structure. Short-range NOE cross peaks between backbone protons were picked up from the ^{15}N 3D NOESY and ^{13}C 3D NOESY spectra. Even with 3D spectra, all the NOE cross peaks could not be assigned straightforwardly to interacting proton pairs because of the degeneracy of the chemical shifts. The pattern of short-range NOE cross peaks showed local structures. Among them, continuous patterns typically seen in α-helices and β-strands were extracted. Strengths obtained from peak heights of short-range NOESY cross peaks and TOCSY peaks are listed in Figure 6.

α-Helices. Five α-helices were determined. First, four α-helices were determined by $NH(i)$–$NH(i+1)$ and medium or weak $C^{\alpha}H(i)$–$NH(i+1)$ connectivities. Short-range NOE $C^{\alpha}H(i)$–$C^{\beta}H(i+3)$, $NH(i)$–$C^{\beta}H(i)$, and $C^{\beta}H(i)$–$NH(i+1)$ cross peaks are also important for determining α-helices definitely. Since assignments of $C^{\beta}H$ protons were not obtained at this stage, the following restriction condition was added instead. The ith residue in α-helices should satisfy the condition that an $C^{\alpha}H(j)$–$NH(j+3)$ ($i = j, j+1$, or $j+2$) or $C^{\alpha}H(j)$–$NH(j+4)$ ($i = j, j+1, j+2$, or $j+3$) NOE connectivity is to be observed. These connectivities should be very weak, but often stronger cross peaks were observed, depending on the relative positions of $C^{\beta}H(j+3)$ and $C^{\beta}H(j+4)$ through which magnetization was transferred indirectly. This restriction was too strong but safer. Because the residue W81 did not satisfy this restriction, the second α-helix was considered as two parts. Finally, five α-helices, N44–A58, Q72–Q80, I82–G89, V101–A110, and E129–M142, were extracted. These elements are indicated in Figure 6.

β-Strands. There were five β-strands characterized by strong $C^{\alpha}H$–NH TOCSY peaks and strong sequential cross peaks between NH and $C^{\alpha}H$ of the preceding residue. In these segments any NOE cross peak, $NH(i)$–$NH(i+1)$, $C^{\alpha}H(i)$–$NH(i+3)$, or $C^{\alpha}H(i)$–$NH(i+4)$, should not be observed. For Gly residues, TOCSY peaks were very weak, and sequential NOESY peaks were also weaker. The chemical shifts of two

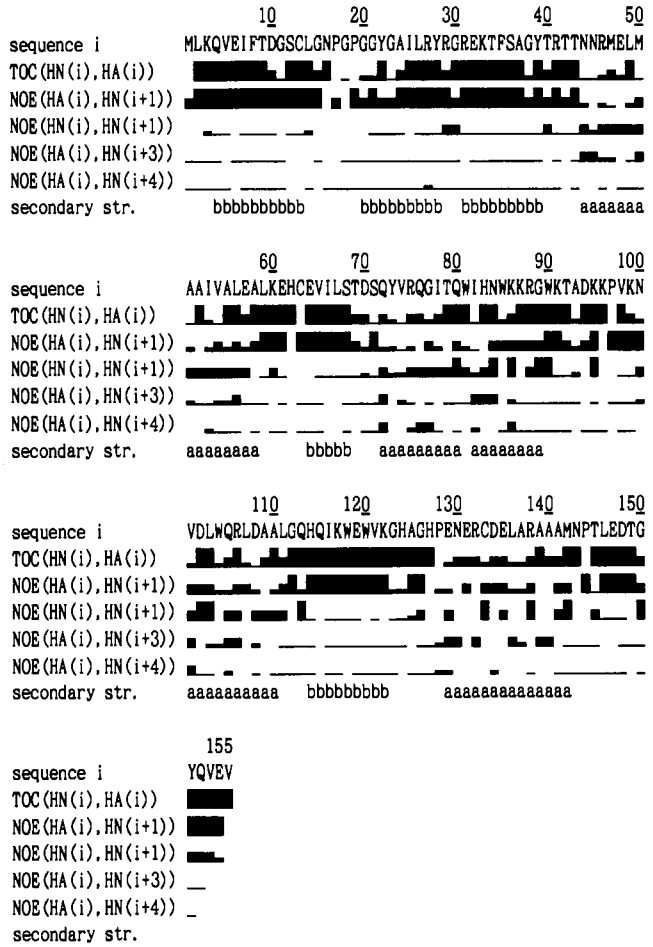

FIGURE 6: Summary of intensities of short-range cross peaks and the estimated secondary structure elements. From the top are shown the intensities of TOCSY cross peaks of NH(i)–C$^\alpha$H(i), NOESY cross peaks of C$^\alpha$H(i)–NH(i+1), NH(i)–NH(i+1), C$^\alpha$H(i)–NH(i+3), and C$^\alpha$H(i)–NH(i+4). The intensities were obtained by reading heights of cross peaks in 2D slices of 3D spectra. The heights of the bars show intensity classification of cross peaks into strong, medium, weak, and zero. Note that the lowest bars indicate the zero level, which means that the cross peak is not observed. Blanks means that no information is available because of degenerate chemical shifts or nonexistent amide protons. The secondary structure elements determined from these results with the criteria explained in the text are shown at the bottom, where the character "a" shows a residue in an α-helix and the character "b" shows a residue in a β-strand.

C$^\alpha$H protons, one of which was below 4 ppm and the other was over 5 ppm, were also used for the decisions. Under the above conditions, five β-strands, Q4–C13, G20–Y28, R31–Y39, E64–S68, and H114–K122, were extracted.

β-Sheet. If two strands make an antiparallel β-sheet, there are NOESY cross peaks between α-protons facing each other. If they make a parallel β-sheet, there are NOESY cross peaks between C$^\alpha$H and NH facing each other. The three strands Q4–C13, G20–Y28, and R31–Y39 formed an antiparallel β-sheet; the strands E64–S68 and H114–K122 ran parallel to the strand Q4–C13. The relative positions of β-strands in the sheet and observed NOEs are summarized in Figure 7. There was another short β-strand, L146–T149. An NOE C$^\alpha$H(Y39)–NH(L146) connectivity was also observed.

Comparison with an X-ray Structure. The solution structure obtained from this NMR study can be compared with a crystal structure recently proposed (Katayanagi et al., 1990). The numbers and positions of secondary structure elements, five α-helices and five β-strands proposed on the basis of NMR data (Figure 6), agree very well with the results given by X-ray crystallography. The topology of the β-sheet has a perfect

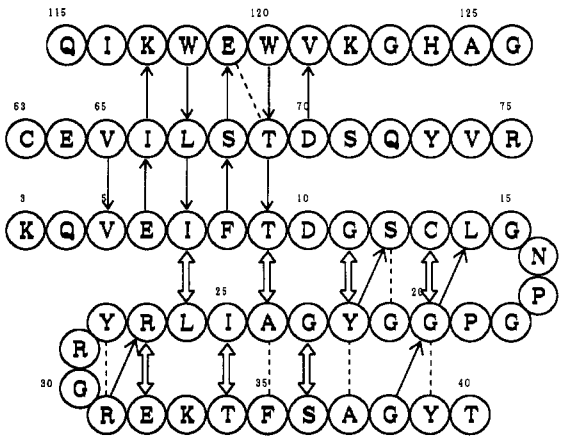

FIGURE 7: Topology of a recognized β-sheet together with observed NOE connectivities. The five β-strands form the core structure of one β-sheet. The outlined arrows show NOE connectivities between C$^\alpha$H protons, the broken lines show NOE connectivities between NH protons, and the solid arrows show directional NOE connectivities from C$^\alpha$H protons to NH's.

coincidence in the two structures. From the result of this comparison, the solution structure, at least the secondary structure, is well conserved in the crystals. However, there seems to be small discrepancies between the two structures: the shortness of two residues of the C-terminal end of the fourth α-helix (L111 and G112) and the shortness of two residues of the N-terminal end of the fifth (H127 and P128). These differences might be attributed to the difference in utilized structural information between two studies rather than to the difference of structures. The NMR structural parameters obtained at this stage are never contradictory to those from the X-ray study. It is well known that α-helix elements can be identified more precisely by NOE cross peaks between C$^\alpha$H(i) and C$^\beta$H(i+3). Our study in progress toward the assignment of side-chain nuclei will reveal a more detailed character of the α-helices.

Reliability of Assignment. A total of 88% of NOE connectivities NH(i)–NH(j) were reported to result in $j = i$+1 or $j = i$–1 (Billeter et al., 1982). This probability is not high enough to assume that all the connectivities arise from the sequential ones, because about 10 mistakes must occur on the average in the intermediate stage of assignment when this assumption is applied to the protein with 155 amino acid residues. Here, we show a new statistical result that the NH–NH NOE connectivity is actually safer to be assigned to the sequential one. In β-sheets, NOE connectivities can be observed not only between sequential residues but also between neighboring strands. To obtain new statistics, we used a new set of proteins (Ponder & Richards, 1987) in the protein data bank, instead of that used by Billeter et al. Secondary structure elements were defined according to the pattern recognition of hydrogen bonds of backbone nuclei (Kabsch & Sander, 1983). The results were as follows: among 1546 pairs of NH protons within a 3.0-Å distance, 88% were in sequential NH's, 10% were between β-strands facing each other, and the remaining of 2% were dangerous pairs. Our sequential assignment procedure can be summarized then as follows: first, residues are identified by strong C$^\alpha$H(i)–NH(i+1) sequential connectivities assigned to be included in β-strands; second, residues are assigned to be sequential ones by NH(i)–NH(i+1) connectivities; and others are assigned by their respective evidence.

The sequential assignment of the backbone resonances of RNase H has been completed by the combination of the selective and nonselective isotope-labeling techniques and five

Table II: Chemical Shifts for Assigned Resonances of Backbone Nuclei, Amide Protons (NH), Amide Nitrogens (N), α-Protons ($C^{\alpha}H$), and α-Carbons (C^{α}) of RNase H from *E. coli* at 27 °C and pH 5.5[a]

residue	N	NH	C^{α}	$C^{\alpha}H$	residue	N	NH	C^{α}	$C^{\alpha}H$	residue	N	NH	C^{α}	$C^{\alpha}H$
M1			53.1	4.17	I53	116.5	7.94		3.13	Q105	115.8	8.42	57.4	3.66
L2	125.1	8.71		4.55	V54	116.5	8.25		3.30	R106	121.0	7.02	57.4	4.18
K3	123.8	8.73	55.1	4.31	A55	119.4	6.85	52.7	3.34	L107	121.6	8.76		4.12
Q4	122.8	8.31	53.3	5.13	L56	112.8	7.57		3.76	D108	118.4	8.76	56.6	4.56
V5	121.8	8.79		4.82	E57	118.4	8.75	56.6	3.94	A109	119.1	7.88	52.9	4.20
E6	124.1	8.64	53.1	4.83	A58	119.6	7.10	51.2	4.11	A110	121.0	7.67	52.7	4.30
I7	121.8	8.60		5.33	L59	118.4	7.15		4.26	L111	117.4	8.68		4.10
F8	128.2	9.13	53.5	5.67	K60	121.8	8.59	53.9	4.38	G112	101.5	7.54	44.4	3.95/4.13
T9	109.5	8.05	58.8	5.61	E61	116.4	7.66	52.2	4.48	Q113	117.2	7.52	53.5	4.27
D10	120.2	9.06	52.7	5.16	H62	119.2	8.46		4.77	H114	116.6	7.37		5.04
G11	106.7	8.70	42.4	3.39/5.04	C63	??	??	57.0	5.12	Q115	120.9	8.48	52.7	4.74
S12	113.5	8.80	55.8	4.78	E64	122.6	8.75	53.7	5.02	I116	125.9	8.57		4.54
C13	123.2	8.44	56.6	4.96	V65	125.6	8.82		4.70	K117	129.8	8.81	52.7	4.48
L14	128.3	9.05		4.49	I66	127.4	8.25		4.75	W118	125.9	8.26	54.1	4.46
G15	107.6	7.82	42.8	3.83/4.11	L67	134.5	8.57		4.70	E119	126.5	8.94	52.5	4.34
N16	116.2	8.24	49.2	5.06	S68	120.8	8.72	54.5	5.73	W120	125.8	7.93	52.0	5.62
P17			61.3	4.92	T69	119.7	8.50	58.6	5.11	V121	123.6	8.03		4.20
G18	105.3	8.32	43.8	3.90/4.30	D70	127.7	8.94	51.2	5.45	K122	124.3	8.46	53.9	4.54
P19			61.3	4.92	S71	115.5	8.31	56.8	4.52	G123	111.3	8.46	43.4	3.91/4.07
G20	108.4	8.96	43.8	3.76/5.07	Q72	132.8	9.37	56.2	3.98	H124	116.5	8.57		4.64
G21	106.5	9.04	44.6	4.22/5.36	Y73	123.6	8.72	59.3	4.48	A125	123.5	8.14	50.8	4.45
Y22	113.3	7.87	53.5	5.74	V74	117.4	8.06		3.60	G126	109.8	8.66	43.4	3.82
G23	106.2	8.99	43.4	3.90/5.17	R75	117.7	7.08	57.4	2.52	H127	118.5	8.40		5.23
A24	126.0	9.52	49.2	5.89	Q76	120.6	8.22	57.0	3.15	P128			63.6	4.39
I125	120.7	9.04		4.88	G77	107.1	7.82	46.1	3.14/3.75	E129	117.8	9.37	59.0	3.63
L26	129.2	9.21		5.29	I78	119.9	8.40		3.73	N130	117.2	7.66	56.6	4.45
R27	127.1	9.98	53.1	5.47	T79	107.4	7.80	62.1	4.11	E131	120.2	7.83	57.8	3.92
Y28	125.2	8.59	54.7	5.06	Q80	117.3	7.53	55.1	4.47	R132	119.8	8.02	57.4	4.09
R29	126.7	9.37	55.1	3.78	W81	118.2	7.10	55.8	4.28	C133	117.8	8.10	63.2	4.01
G30	104.9	8.72	43.6	3.61/4.14	I82	117.9	8.48		3.49	D134	120.8	7.78	55.3	4.46
R31	121.0	7.95	52.9	4.69	H83	118.4	7.93		4.13	E135	118.9	7.83	57.8	3.92
E32	122.7	8.76	53.1	5.43	N84	117.7	7.44	53.5	4.38	L136	120.1	8.30		4.02
K33	125.0	9.21	53.1	4.67	W85	120.3	8.20	55.8	4.38	A137	122.7	8.35	53.5	3.62
T34	114.5	8.14	58.2	5.32	K86	119.0	8.12	58.2	2.70	R138	116.5	8.24	57.6	3.80
F35	120.6	9.31	54.5	4.99	K87	119.0	7.36	56.6	4.09	A139	120.4	7.89	52.9	4.04
S36	113.9	8.40	56.2	4.58	R88	116.3	7.24	53.1	4.48	A140	121.8	7.88	52.7	3.98
A37	120.8	6.37	50.2	4.25	G89	108.7	7.78	45.3	3.93	A141	119.2	7.79	52.7	3.75
G38	106.2	8.58	42.2	3.49/5.36	W90	112.8	8.56	56.2	3.42	M142	111.0	7.11	53.9	4.29
Y39	122.8	9.69	53.9	5.47	K91	116.7	6.82	52.0	5.05	N143	117.0	7.42	49.4	5.04
T40	113.5	8.81	63.6	3.73	T92	109.6	8.90	59.0	4.38	P144			62.1	4.10
R41	119.9	7.77	55.1	3.88	A93	123.6	9.10	53.1	4.07	T145	108.4	7.49	59.3	4.56
T42	125.0	8.85	58.0	4.08	D94	114.0	8.00	51.2	4.64	L146	123.4	8.08		4.76
T43	106.5	8.53	57.0	5.28	K95	112.5	8.06	55.8	3.67	E147	117.9	8.35	52.5	4.82
N44	120.6	9.19	56.0	3.92	K96	119.8	7.62	51.6	4.72	D148	125.6	10.04	50.4	4.88
N45	116.3	8.56	53.9	4.03	P97			60.9	4.61	T149	116.6	7.88	62.5	4.14
R46	116.5	7.38	59.0	3.58	V98	120.7	7.57		3.44	G150	106.7	8.02	43.0	3.73/4.21
M47	118.2	7.71	55.5	4.44	K99	127.9	8.29	55.5	4.05	Y151	121.4	7.27	56.8	4.24
E48	119.3	8.44	57.8	3.86	N100	115.8	9.45	53.1	4.28	Q152	126.0	7.60	52.3	4.15
L49	116.1	7.24		3.96	V101	119.0	7.65		3.60	V153	120.6	7.86		3.84
M50	118.7	8.69	55.5	3.93	D102	119.0	8.59	54.3	4.09	E154	125.2	8.26	54.5	4.34
A51	117.0	7.72	53.3	3.31	L103	118.6	7.28		4.16	V155	125.4	7.73		4.04
A52	113.7	6.47	52.7	3.99	W104	121.0	8.55	59.3	4.56					

[a] The chemical shifts are relative to TMS for ^{1}H, TMS for ^{13}C, and liquid NH_3 for ^{15}N, respectively. The accuracy of chemical shifts of C^{α}'s is ±0.2 ppm, that of protons is ±0.01 ppm, and that of nitrogens is ±0.1 ppm. The chemical shifts of C^{α}'s of His, Val, Ile, and Leu residues were not yet obtained. NH of C63 was not observed.

types of heteronuclear 3D NMRs and assisting 2D NMRs. We summarize the factors that contributed to the success of this approach. (1) The 3D NMRs have enough resolving power for a 155-residue protein. (2) The 3D NMRs have enough sensitivity for 2 mM samples. (3) The five 3D NMRs compensate for each other to complete the sequential connectivities. (4) Amino acid type identification by ^{15}N selective labelings are reliable and inexpensive.

Conclusion

The assignment of resonance peaks of the backbone nuclei in a 155-residue protein, RNase H from *E. coli* was successfully performed, and its secondary structure was elucidated. The structure determined by NMR agrees well with that obtained from an X-ray crystallographic study. The experimental and analytical procedures proposed in this article are applicable to proteins of a comparable size, even on a widely utilized 400-MHz machine equipped with two radio frequency channels. The development of multidimensional NMR experiments will make it possible to elucidate the tertiary structures of proteins larger than 20 kDa.

Acknowledgments

We thank Chieko Katsuta for help with the fermentation, Dr. Yasushi Oda for useful discussions, and Drs. Katsuo Katayanagi and Kosuke Morikawa for discussions on the structure of RNase H.

Registry No. RNase H, 9050-76-4.

References

Bax, A., Griffey, R. H., & Hawkins, B. L. (1983) *J. Magn. Reson. 55*, 301–315.

Bax, A., Ikura, M., Kay, L. E., Torchia, D. A., & Tschudin, R. (1990) *J. Magn. Reson. 86*, 304–318.
Billeter, M., Braun, W., & Wüthrich, K. (1982) *J. Mol. Biol. 155*, 321–346.
Crouch, R. J., & Dirksen, M.-L. (1982) in *Nucleases* (Linn, S. M., & Roberts, R. J., Eds.) pp 211–241, Cold Spring Harbor Laboratory, Cold Spring Harbor, NY.
Davis, D. (1989) *J. Magn. Reson. 81*, 603–607.
Driscoll, P. C., Clore, G. M., Marion, D., Wingfield, P. T., & Gronenborn, A. M. (1990) *Biochemistry 29*, 3542–3556.
Fesik, S. W., & Zuiderweg, E. R. P. (1988) *J. Magn. Reson. 78*, 588–593.
Griesinger, C., Sørensen, O. W., & Ernst, R. R. (1987a) *J. Magn. Reson. 73*, 574–579.
Griesinger, C., Sørensen, O. W., & Ernst, R. R. (1987b) *J. Am. Chem. Soc. 109*, 7227–7228.
Griffey, R. H., Redfield, A. G., Loomis, R. E., & Dahlquist, F. W. (1985a) *Biochemistry 24*, 817–822.
Griffey, R. H., Jarema, M. A., Kuntz, S., Rosevear, P. R., & Redfield, A. G. (1985b) *J. Am. Chem. Soc. 107*, 711–712.
Ikura, M., Kay, L. E., & Bax, A. (1990a) *Biochemistry 29*, 4659–4667.
Ikura, M., Marion, D., Kay, L. E., Shih, H., Krinks, M., Klee, C. B., & Bax, A. (1990b) *Biochem. Pharmacol. 40*, 153–160.
Ikura, M., Bax, A., Clore, M., & Gronenborn, A. M. (1990c) *J. Am. Chem. Soc. 112*, 9020–9022.
Kabsch, W., & Sander, C. (1983) *Biopolymers 22*, 2577–2637.
Kainosho, M., & Tsuji, T. (1982) *Biochemistry 21*, 6273–6279.
Kanaya, S., & Crouch, R. J. (1983) *J. Biol. Chem. 258*, 1276–1281.
Kanaya, S., Kohara, A., Miyagawa, M., Matsuzaki, T., Morikawa, K., & Ikehara, M. (1989) *J. Biol. Chem. 264*, 11546–11549.
Kanaya, S., Kohara, A., Miura, Y., Sekiguchi, A., Iwai, S., Inoue, H., Ohtsuka, E., & Ikehara, M. (1990) *J. Biol. Chem. 265*, 4615–4621.
Katayanagi, K., Miyagawa, M., Matsushima, M., Ishikawa, M., Kanaya, S., Ikehara, M., Matsuzaki, T., & Morikawa, K. (1990) *Nature 347*, 306–309.
Kuroda, Y., Wada, A., Yamazaki, T., & Nagayama, K. (1989) *J. Magn. Reson. 84*, 604–610.
Marion, D., Kay, L. E., Sparks, S. W., Torchia, D. A., & Bax, A. (1989a) *J. Am. Chem. Soc. 111*, 1515–1517.
Marion, D., Driscoll, P. C., Kay, L. E., Wingfield, P. T., Bax, A., Gronenborn, A. M., & Clore, G. M. (1989b) *Biochemistry 28*, 6150–6156.
McIntosh, L. P., Wand, A. J., Lowry, D. F., Redfield, A. G., & Dahlquist, F. W. (1990) *Biochemistry 29*, 6341–6362.
Morris, G. A., & Freeman, R. (1978) *J. Magn. Reson. 29*, 433–462.
Nagayama, K., Yamazaki, T., Yoshida, M., Kanaya, S., & Nakamura, H. (1990) *J. Biochem. 108*, 149–152.
Norwood, T. J., Boyd, J., Heritage, J. E., Soffe, N., & Campbell, I. D. (1990) *J. Magn. Reson. 87*, 488–501.
Oschkinat, H., Griesinger, C., Kraulis, P. J., Sørensen, O. W., Ernst, R. R., Gronenborn, A. M., & Clore, G. M. (1988) *Nature 332*, 374–376.
Ponder, J. W., & Richards, F. M. (1987) *J. Mol. Biol. 193*, 775–791.
Sklenár, V., & Bax, A. (1987) *J. Magn. Reson. 74*, 469–479.
Stein, H., & Hausen, P. (1969) *Science 166*, 393–395.
Takahashi, S., & Nagayama, K. (1988) *J. Magn. Reson. 76*, 347–351.
Torchia, D. A., Sparks, S. W., & Bax, A. (1988) *Biochemistry 27*, 5135–5141.
Torchia, D. A., Sparks, S. W., & Bax, A. (1989) *Biochemistry 28*, 5509–5524.
Vuister, G. W., Boelens, R., & Kaptein, R. (1988) *J. Magn. Reson. 80*, 176–185.
Vuister, G. W., de Waard, P., Boelens, R., Vliegenthart, J. F. G., & Kaptein, R. (1989) *J. Am. Chem. Soc. 111*, 772–774.
Wüthrich, K. (1986) *NMR of Proteins and Nucleic Acids*, John Wiley & Sons, NY.
Yang, W., Hendrickson, W. A., Crouch, R. J., & Satow, Y. (1990) *Science 249*, 1398–1405.
Zuiderweg, E. R. P., & Fesik, S. W. (1989) *Biochemistry 28*, 2387–2391.